

Percolation of a general network of networks

Jianxi Gao,^{1,2} Sergey V. Buldyrev,³ H. Eugene

Stanley,² Xiaoming Xu,¹ and Shlomo Havlin,⁴

¹*Department of Automation, Shanghai Jiao Tong University,
800 Dongchuan Road, Shanghai 200240, PR China*

²*Center for Polymer Studies and Department of Physics,
Boston University, Boston, MA 02215 USA*

³*Department of Physics, Yeshiva University, New York, NY 10033 USA*

⁴*Department of Physics, Bar-Ilan University, 52900 Ramat-Gan, Israel*

(Dated: 15 June 2013 — gbsh061513.tex)

Abstract

Percolation theory is an approach to study vulnerability of a system. We develop analytical framework and analyze percolation properties of a network composed of interdependent networks (NetONet). Typically, percolation of a single network shows that the damage in the network due to a failure is a continuous function of the fraction of failed nodes. In sharp contrast, in NetONet, due to the cascading failures, the percolation transition may be discontinuous and even a single node failure may lead to abrupt collapse of the system. We demonstrate our general framework for a NetONet composed of n classic Erdős-Rényi (ER) networks, where each network depends on the same number m of other networks, i.e., a random regular network of interdependent ER networks. In contrast to a *treelike* NetONet in which the size of the largest connected cluster (mutual component) depends on n , the loops in the RR NetONet cause the largest connected cluster to depend only on m . We also analyzed the extremely vulnerable feedback condition of coupling. In the case of ER networks, the NetONet only exhibits two phases, a second order phase transition and collapse, and there is no first phase transition regime unlike the no feedback condition. In the case of NetONet composed of RR networks, there exists a first order phase transition when q is large and second order phase transition when q is small. Our results can help in designing robust interdependent systems.

PACS numbers:

I. INTRODUCTION

Network science has attracted much attention in recent years due to its interdisciplinary applications [1–21]. Many network results have been obtained by analyzing isolated networks, but most real-world networks do in fact interact with and depend on other networks [3–5, 18, 19]. Thus, in analogy to the ideal gas laws that are valid only in the limiting case that molecules do not interact, so the extensive results for the case of non-interacting networks hold only when it is justified to neglect the interactions between networks. Recently several studies have addressed the resilience as well as other properties of interacting networks [22–41]. A framework based on percolation theory has been developed to analyze the cascading failures caused by interdependencies between two networks [22, 23]. In interdependent networks, when nodes in one network fail they usually cause the failure of dependent nodes in other networks, and this in turn can cause further damage to the first network and result in cascading failures, which could lead to abrupt collapse of the system. Later on, two important generalizations of the basic model [22, 23] have been developed. Because in real-world scenarios the initial failure of important nodes (“hubs”) may not be random but targeted, a mathematical framework for understanding the robustness of interdependent networks under an initial targeted attack on specific degree of nodes has been studied by Huang et al. [24] and later extended by Dong et al. [25]. Also in real-world scenarios, the assumption that each node in network A depends on one and only one node in network B and vice versa may not be valid. To release this assumption, a theoretical framework for understanding the robustness of interdependent networks with a random number of support and dependency relationships has been developed and studied by Shao et al. [26]. More recently, Gao et al. developed an analytical framework to study percolation of a tree-like network formed by n interdependent networks [27–29]. Gao et al. found that while for $n = 1$ the percolation transition is a second order, for any $n > 1$ cascading failures occur and the network collapses as in a first order transition. Indeed cascading failures have caused black-outs in interdependent communication and power grid systems spanning several countries [3, 42]. To be able to design resilient infrastructures or improve existing infrastructures we need to understand how vulnerability is affected by such interdependencies [3–5, 30, 38].

Here we generalize the theory of interdependent networks [27–29] to regular and random regular (RR) network of n interdependent networks that include loops. Figures 1(a) and

1(b) illustrate such network of networks (NetONet), in which each network depends on the same number m of other networks. We develop an exact analytical approach for percolation of a regular and a random regular NetONet system composed of n partially interdependent networks. We show that for an RR network with degree m of n interdependent networks where each network has the same degree distribution, same average degree $\langle k \rangle$ and the fraction of dependence nodes between a pair of interdependent networks, q , is the same for all pairs, the number of networks is irrelevant. We obtain analytically the fraction of survived nodes in each network after cascading failures, P_∞ as a function of p , m and $\langle k \rangle$.

II. CASCADING FAILURES IN A NETWORK OF NETWORKS

A. The Model

In our model, each node in the NetONet is itself a network and each link represents a *fully* or *partially* dependent pair of networks [see Fig. 1]. We assume that each network i ($i = 1, 2, \dots, n$) of the NetONet consists of N_i nodes linked together by connectivity links. Two networks i and j form a partially dependent pair if a certain fraction $q_{ji} > 0$ of nodes in network i directly depend on nodes in network j , i.e., nodes in network i cannot function if the corresponding nodes in network j do not function. A node in a network i will not function if it is removed or if it does not belong to the largest connected cluster (giant component) in network i . Dependent pairs may be connected by unidirectional dependency links pointing from network j to network i [see Fig. 1(c)]. This convention indicates that nodes in network i may get a crucial support from nodes in network j , e.g., electric power if network j is a power grid.

We assume that after an attack or failure only a fraction of nodes p_i in each network i remains. We also assume that only nodes that belong to a giant component in each network i will remain functional. When a cascade of failures occurs, nodes in network i that do not belong to the giant component in network i fail and cause nodes in other networks that depend on them to also fail. When those nodes fail, dependent nodes and isolated nodes in the other networks also fail, and the cascade can cause further failures back in network i . In order to determine the fraction of nodes $P_{\infty,i}$ in each network that remains functional (i.e., the fraction of nodes that constitutes the giant component) after the cascade of failures as

a function of p_i and q_{ij} , we need to analyze the dynamics of the cascading failures.

B. Dynamic Processes

We assume that all N_i nodes in network i are randomly assigned a degree k from a probability distribution $P_i(k)$, they are randomly connected, and the only constraint is that a node with degree k has exactly k links [43]. We define the generating function of the degree distribution,

$$G_i(z) \equiv \sum_{k=0}^{\infty} P_i(k) z^k, \quad (1)$$

where z is an arbitrary complex variable. The generating function of this branching process is defined as $H_i(z) \equiv G'_i(z)/G'_i(1)$. Once a fraction $1 - x$ of nodes is randomly removed from a network, the probability that a randomly chosen node belongs to a giant component, is given by [22, 23, 44–47]

$$g_i(x) = 1 - G_i[xf_i(x) + 1 - x], \quad (2)$$

where $f_i(x)$ satisfies

$$f_i(x) = H_i[xf_i(x) + 1 - x]. \quad (3)$$

We assume that (i) each node a in network i depends with a probability q_{ji} on only one node b in network j , and that, (ii) if node a in network i depends on node b in network j and node b in network j depends on node c in network i , then node a coincides with node c , i.e., we have a no-feedback situation [29]. In section IV we study the case of feedback condition, i.e., node a can be different from c in network i . The no feedback condition prevents configurations from collapsing even without having their internal connectivity in each network [26]. Next, we develop the dynamic process of cascading failures step by step.

At $t = 1$, in networks i of the NetONet we randomly remove a fraction $1 - p_i$ of nodes. After the initial removal of nodes, the remaining fraction of nodes in network i , is $\psi'_{i,1} \equiv p$. The remaining functional part of network i therefore constitutes a fraction $\psi_{i,1} = \psi'_{i,1} g_A(\psi'_{i,1})$ of the network nodes, where $g_i(\psi'_{i,1})$ is defined by Eqs. (2) and (3). Furthermore, we denote by $y_{ji,1}$ the fraction of nodes in network i that survive after the damage from all the networks connected to network i except network j is taken into account, so if $q_{ij} \neq 0$, $y_{ji,1} = p_j$.

When $t \geq 2$, all the networks receive the damages from their neighboring networks one by one. Without loss of generality, we assume that network 1 is the first, network 2 second,..., and network n is last. In Fig. 1(c), for example, since a fraction q_{21} , q_{31} , q_{41} and q_{71} of nodes of network 1 depends on nodes from network 2, 3, 4 and 7 respectively, the remaining fraction of network 1 nodes is,

$$\psi'_{1,t} = \prod_{j=2,3,4,7} [q_{j1}y_{j1,t-1}g_j(\psi'_{j,t-1}) - q_{j1} + 1], \quad (4)$$

and $y_{1j,t}$ ($j = 2, 3, 4, 7$) satisfies

$$y_{1j,t} = \frac{\psi'_{1,t}}{q_{j1}y_{j1,t-1}g_j(\psi'_{j,t-1}) - q_{j1} + 1}. \quad (5)$$

The remaining functional part of network 1 therefore contains a fraction $\psi_{1,t} = \psi'_{1,t}g_1(\psi'_{1,t})$ of the network nodes.

Similarly, we obtain the remaining fraction of network i nodes,

$$\psi'_{i,t} = \prod_{j<i} [q_{ji}y_{ji,t-1}g_j(\psi'_{j,t}) - q_{ji} + 1] \prod_{s>i} [q_{si}y_{si,t-1}g_s(\psi'_{s,t-1}) - q_{si} + 1], \quad (6)$$

and $y_{ij,t}$ is

$$y_{ij,t} = \frac{\psi'_{i,t}}{q_{ji}y_{ji,t-1}g_j(\psi'_{j,t}) - q_{ji} + 1}, \quad (7)$$

and $y_{is,t}$ is

$$y_{is,t} = \frac{\psi'_{i,t}}{q_{si}y_{si,t-1}g_s(\psi'_{s,t-1}) - q_{si} + 1}. \quad (8)$$

Following this approach we can construct the sequence, $\psi'_{i,t}$ of the remaining fraction of nodes at each stage of the cascade of failures. The general form is given by

$$\begin{aligned} \psi'_{i,1} &\equiv p_i, \\ y_{ij,1} &\equiv p_i, q_{ij} \neq 0 \\ \psi'_{i,t} &= p_i \prod_{j<i} [q_{ji}y_{ji,t-1}g_j(\psi'_{j,t}) - q_{ji} + 1] \prod_{s>i} [q_{si}y_{si,t-1}g_s(\psi'_{s,t-1}) - q_{si} + 1], \\ y_{ij,t} &= \frac{\psi'_{i,t}}{q_{ji}y_{ji,t-1}g_j(\psi'_{j,t}) - q_{ji} + 1}, \\ y_{is,t} &= \frac{\psi'_{i,t}}{q_{si}y_{si,t-1}g_s(\psi'_{s,t-1}) - q_{si} + 1}. \end{aligned} \quad (9)$$

We compare the theoretical formulas of the dynamics, Eqs. (9) and simulation results in Fig. 2. As seen the theory of the dynamics (9) agrees well with simulations.

C. Stationary State

To determine the state of the system at the end of the cascade process we look at $\psi'_{i,\tau}$ at the limit of $\tau \rightarrow \infty$. This limit must satisfy the equations $\psi'_{i,\tau} = \psi'_{i,\tau+1}$ since eventually the clusters stop fragmenting and the fractions of randomly removed nodes at step τ and $\tau + 1$ are equal. Denoting $\psi'_{i,\tau} = x_i$, we arrive for the n networks, at the stationary state, to a system of n equations with n unknowns,

$$x_i = p_i \prod_{j=1}^K (q_{ji} y_{ji} g_j(x_j) - q_{ji} + 1), \quad (10)$$

where the product is taken over K networks interlinked with network i by partial (or fully) dependency links [see Fig. 1] and

$$y_{ij} = \frac{x_i}{q_{ji} y_{ji} g_j(x_j) - q_{ji} + 1}, \quad (11)$$

is the fraction of nodes in network i that survive after the damage from all the networks connected to network j except network i itself is taken into account. The damage from network i itself is excluded due to the no-feedback condition. Equation (10) is valid for any type of interdependent NetONet, while Eqs. (11) represents the no-feedback condition. For two coupled networks, Eqs. (10) and (11) are equivalent to Eq. (13) of Ref. [26] for the specific case of single dependency links.

Our general framework for percolation of interdependent network of networks, Eqs. (10) and (11), can be generalized in two directions: (i) coupling with feedback condition (ii) coupling with multiple-support.

(i) In the existence of the feedback, $y_{i,j}$ is simply x_i and Eqs. (10) and (11) become a single equation,

$$x_i = p_i \prod_{j=1}^K (q_{ji} x_j g_j(x_j) - q_{ji} + 1). \quad (12)$$

The feedback condition leads to an extreme vulnerability of the network of interdependent networks. As we know for two fully interdependent networks with no-feedback condition [22] if the average degree is large enough both networks exist. However, for two fully interdependent networks with feedback condition, no matter how large the average degree is, both networks collapse even after a single node is removed. The analytical results about the feedback condition are given in section IV.

(ii) Equation (10) can be generalized to the case of multiple dependency links studied for a pair of coupled networks in [26] by,

$$x_i = p_i \prod_{j=1}^K (1 - q_{ji} G^{ji} [1 - x_j g_j(x_j)]) , \quad (13)$$

where G^{ji} represents the generating function of the degree distribution of multiple support links that network i depends on network j .

On one hand, the term g_i reflects the topology of network i , which can be an ER network, a RR network, a scale free (SF) network, or even a small world (SW) network. On the other hand, $Q = [q_{ij}]_{n \times n}$ (n is the number of networks) reflects the interactions between the networks, i.e., the topology of the NetONet, which can also be any type of network. Our theoretical results Eq. (10) and (11) are therefore general for any type of network of networks. By solving Eqs. (10) and (11), or Eqs. (12), or Eqs. (13), we obtain x_i of each network for coupled networks with no feedback condition, feedback condition and multiple-support condition, respectively. Thus, we obtain the giant component in each network i as

$$P_{\infty,i} \equiv x_i g_i(x_i). \quad (14)$$

III. NO FEEDBACK CONDITION

A. The general case of an RR NetONet formed of random networks.

In order to study the various forms the stationary state of the system can reach after a cascading failure, we first assume, without loss of generality, that each network depends on m other random networks, i.e., that we have a RR network formed of n random networks. We understand the RR category to also include regular non-random networks in which each network has the same number of neighbouring interdependent networks with a structure e.g., of a lattice of ER networks [Fig. 1(a)]. We assume, for simplicity, that the initial attack on each network is by removing randomly a fraction $1 - p$ of nodes, the partial interdependency fraction is q , and the average degree of each ER network is the same \bar{k} for all networks. Because of the symmetries involved, the $nm + m$ equations in Eqs. (10) and (11) can be

reduced to two equations,

$$\begin{cases} x = p(qyg(x) - q + 1)^m, \\ y = p(qyg(x) - q + 1)^{m-1}. \end{cases} \quad (15)$$

By substituting $z = xf(x) + 1 - x$, Eqs. (2), (3) and (14) into (15), and eliminating f , x , and y , we obtain

$$P_\infty(z) = \frac{[1 - G(z)](1 - z)}{1 - H(z)}, \quad (16)$$

and

$$\left(\frac{1 - z}{1 - H(z)}\right)^{\frac{1}{m}} \left(\frac{1}{p}\right)^{\frac{2}{m}} + (q - 1) \left(\frac{1}{p}\right)^{\frac{1}{m}} - qP_\infty(z) \left(\frac{1 - H(z)}{1 - z}\right)^{\frac{1}{m}} = 0. \quad (17)$$

Equation (17) can help us to understand the percolation of a RR network of any inter-dependent random networks where all networks have the same average degree and degree distribution.

To solve Eq. (17), we introduce an analytical function $R(z)$ for $z \in [0, 1]$ as

$$\frac{1}{p} = \frac{H(z) - 1}{z - 1} \left(\frac{1 - q + \sqrt{(1 - q)^2 + 4qP_\infty(z)}}{2} \right)^m \equiv R(z). \quad (18)$$

$R(z)$ as a function of z has a quite complex behaviour for various degree distributions. We present two examples to demonstrate our general results on (i) RR network of ER networks and (ii) RR network of SF networks.

- (i) For the case of RR network of ER networks we find a critical q_c such that, when $q < q_c$ the system shows a second order phase transition and the critical threshold p_c depends on q and average degree \bar{k} . When $q_c < q < q_{\max}$ the system shows a first order phase transition, and when $q > q_{\max}$ there is no phase transition because all the networks collapse even for a single node failure.
- (ii) For the case of RR network of SF networks, the phase diagram is different from the ER case, because there is no pure first order phase transition. However, there exists an effective q_c^e , when $q < q_c^e$, the system shows a second order phase transition and the critical threshold is $p_c = 0$ for infinite number of nodes in each network, i.e., the maximum degree goes to ∞ . When $q_c^e < q < q_{\max}$, the system shows a hybrid

transition as follows. When p decreases from 1 to 0, the giant component P_∞ as function of p shows a sharp jump at p_{ec}^I , which is like a first order transition to a finite small value, and then (when p further decreases) goes smoothly to 0. For $q > q_{\max}$ there is no phase transition because all the networks collapse even for a single node failure.

B. RR network formed by interdependent ER networks

For ER networks [48–50], the generating function $g(x)$ satisfies [44–47]

$$\begin{aligned} g(x) &= 1 - \exp[\bar{k}x(f - 1)], \\ f &= \exp[\bar{k}x(f - 1)]. \end{aligned} \quad (19)$$

Substituting Eqs. (19) into Eqs. (15), we get

$$\begin{aligned} f &= \exp\{\bar{k}p[qy(1 - f) - q + 1]^m(f - 1)\}, \\ y &= p[qy(1 - f) - q + 1]^{m-1}, \\ P_\infty &= -(\log f)/\bar{k}. \end{aligned} \quad (20)$$

Eliminating y from Eq. (20), we obtain an equation for f ,

$$\left[\frac{\ln f}{\bar{k}p(f-1)}\right]^{\frac{2}{m}} + (q-1)\left[\frac{\ln f}{\bar{k}p(f-1)}\right]^{\frac{1}{m}} + \frac{q}{\bar{k}} \log f = 0. \quad (21)$$

Considering $[\ln f/\bar{k}p(f-1)]^{1/m}$ to be a variable, Eq. (21) becomes a quadratic equation that can be solved analytically having only one valid solution,

$$2^m \ln f = \bar{k}p(f-1) \left[1 - q + \sqrt{(1-q)^2 - \frac{4q}{\bar{k}} \ln f}\right]^m. \quad (22)$$

From Eq. (22) and the last equation in (20), we determine the mutual percolation giant component for a RR network of ER networks,

$$P_\infty = \frac{p}{2^m} (1 - e^{-\bar{k}P_\infty}) \left[1 - q + \sqrt{(1-q)^2 + 4qP_\infty}\right]^m. \quad (23)$$

Figures 3(a) and 3(b) show numerical solutions of Eq. (23) for several q and m values compared with simulations. These solutions imply that P_∞ as a function of p exhibits a second (continuous) or a first order (abrupt) phase transition depending on the values of q and m for a given \bar{k} . Note, when $q=0$ or $m=0$, Eq. (23) is reduced to the known equation, $P_\infty = p(1 - e^{-\bar{k}P_\infty})$, for single ER networks [48–50].

From Eqs. (18) and (23), we obtain

$$R(z) = \frac{1}{p} = \frac{(1 - e^{\bar{k}(z-1)})[1 - q + \sqrt{(1-q)^2 + 4q(1-z)}]^m}{2^m(1-z)}, \quad (24)$$

and

$$F(z) \equiv \frac{dR(z)}{dz} = \frac{e^{\bar{k}(1-z)} - \bar{k}(1-z)}{p(1-z)(e^{\bar{k}(1-z)} - 1)} - \frac{2mq}{p[1 - q + \sqrt{(1-q)^2 + 4q(1-z)}]\sqrt{(1-q)^2 + 4q(1-z)}}. \quad (25)$$

Next we demonstrate the behaviour of Eq. (24) as shown in Fig. 4. For given \bar{k} and m , when q is small, $R(z)$ is a monotonously increasing function of z , for example see the curve for $q = 0.42$. Thus, the maximum of $R(z)$ is obtained when $z \rightarrow 1$, which corresponds to a second order phase transition threshold $p_c^{II} = 1/\max\{R(z)\} \equiv 1/R(z_c)$, where $P_\infty(p_c^{II}) = 1 - z_c = 0$. When q increases, $R(z)$ as a function of z shows a maxima at $z < 1$ and $\max\{R(z)\} > 1$, for example for $q = 0.50$ in Fig. 4. Thus, the maximum of $R(z)$ is obtained when $z = z_c \in (0, 1)$ at the peak, which corresponds to the first order phase transition threshold $p_c^I = 1/\max\{R(z)\} = 1/R(z_c)$, where $P_\infty(p_c^I) = 1 - z_c > 0$. The q value in which for the first time a maxima of $R(z)$ appears at $z < 1$ is q_c , the critical dependency which separates between the first and second order transitions. When q continually further increases, $\max\{R(z)\} < 1$, which corresponds to a complete collapse of the NetONet. The value of q for which $\max\{R(z)\} = 1$ is q_{max} , above which the network is not stable and collapse instantaneously.

Next we analyze the different behaviours of RR network of ER networks in the different regimes of q : (i) For $q < q_c$, the percolation is a continuous second order which is characterized by a critical threshold p_c^{II} . (ii) The range of $q_c < q < q_{max}$ is characterized by an abrupt first order phase transition with a critical threshold p_c^I . (iii) For $q > q_{max}$ no transition exists due to the instant collapse of the system.

We next analyze in detail the parameters characterizing the three regimes. (i) For a given m and \bar{k} , when q is sufficiently small, there exists a critical p_c^{II} such that, when p increases above p_c^{II} , P_∞ continuously increases from zero to non-zero values. Here P_∞ as a function of p exhibits a second order phase transition. In order to get p_c^{II} we analyze Eq. (25). When q is sufficiently small $\frac{dR(z)}{dz} > 0$, the maximum value of $R(z)$ is obtained when $z \rightarrow 1$. Thus, we obtain the critical threshold for the second order phase transition, p_c^{II} by substituting

$z \rightarrow 1$ into Eq. (24),

$$p_c^{II} = \frac{1}{\bar{k}(1-q)^m}. \quad (26)$$

(ii) Next we obtain p_c^I . According to Eq. (25), when q increases, $R(z)$ as a function z becomes not monotonous and a maxima appears, which corresponds to the condition for first order phase transition, i.e., when $\frac{dR(z)}{dz} = 0$. Furthermore, for a given p , the smallest of these roots gives the physically meaningful solution from which the giant component $0 < P_\infty(p_c) < 1$ can be found from Eq. (23).

By solving z_c from $F(z_c) = 0$ of Eq. (25), we obtain the critical threshold for first order phase transition p_c^I as

$$p_c^I = \frac{2^m(1-z_c)}{(1-e^{\bar{k}(z_c-1)})(1-q+\sqrt{(1-q)^2+4q(1-z_c)})^m}. \quad (27)$$

Next we study the critical coupling strength q_c , i.e, the critical coupling that distinguishes between first and second order transitions. We find that P_∞ undergoes a second order transition as a function of p when $q < q_c$, a first order transition when $q_c < q < q_{\max}$, and no phase transition (the system is unstable for any p) when $q > q_{\max}$. By definition, when a system changes from second order to first order at the critical point, q , m , and \bar{k} satisfy $p_c^I = p_c^{II}$, i.e., both conditions for the first order and second order phase transition should satisfy,

$$\lim_{z \rightarrow 1} \frac{dR(z)}{dz} = 0. \quad (28)$$

From Eqs. (25) and (28), we obtain

$$2qm - \bar{k}(1-q)^2 = 0. \quad (29)$$

Solving Eq. (29), we find that the physically meaningful q_c is

$$q_c = \frac{\bar{k} + m - (m^2 + 2\bar{k}m)^{1/2}}{\bar{k}}. \quad (30)$$

(iii) Next we calculate the critical point q_{\max} , above which ($q > q_{\max}$) the system is unstable for any p . From Eq. (24), the system is unstable for any p , when $R(z) \leq 1$. We therefore, can obtain q_{\max} by satisfying Eq. (25) and $p_c^I = 1$. Thus, we obtain q_{\max} as

$$q_{\max} = \frac{(a^{1/m} - 1)^2}{2(1 - 2z_c - a^{1/m})}, \quad (31)$$

where a satisfies

$$a = \frac{1 - e^{\bar{k}(z_c - 1)}}{2^m(1 - z_c)}, \quad (32)$$

and z_c can be solved by substituting Eq. (31) into Eq. (25) and set $p = 1$, $F(z_c) = 0$, which is one equation with only one unknown z_c .

Next we obtain the numerical solution of $P_\infty(p_c)$ as a function q as shown in Fig. 5. From Fig. 5, we can see that for fixed m and \bar{k} , there exist two critical values of coupling strength, q_c and q_{\max} , when $q < q_c$, $P_\infty(p_c) = 0$ which represents a second order phase transition, when $q_c < q < q_{\max}$, $P_\infty(p_c) > 0$ representing a first order phase transition. When $q > q_{\max}$, $P_\infty(p_c) = 0$ representing the NetONet collapse and that there is no phase transition ($p_c = 1$). Figure 6 shows the phase diagram of RR network of ER networks for different values of m and \bar{k} . As m decreases and k increases, the region for $P_\infty > 0$ increases, which shows a better robustness.

C. The case of RR NetONet formed of interdependent scale-free (SF) networks.

We analyze here NetONets composed of SF networks with a power law degree distribution $P(k) \sim k^{-\lambda}$. The corresponding generating function is

$$G(z) = \frac{\sum_s^M [(k+1)^{1-\lambda} - k^{1-\lambda}] z^k}{(M+1)^{1-\lambda} - s^{1-\lambda}} \quad (33)$$

where s ($s = 2$ in this paper) is the minimal degree cutoff and M is the maximal degree cutoff.

SF networks approximate real networks such as the Internet, airline flight patterns, and patterns of scientific collaboration [6, 51–53]. When SF networks are fully interdependent [22], $p_c > 0$, even in the case $\lambda \leq 3$ in contrast to a single network for which $p_c = 0$ [7]. We study the percolation of a RR network composed of interdependent SF networks by substituting their degree distribution into Eq. (1) and obtaining their generating functions. We assume, for simplicity, that all the networks in the NetONet have the same λ , s and M , and use Eq. (17) to analyze the percolation of an RR NetONet of SF networks.

The generating function of the branching process is defined as $H(z) = G'(z)/G'(1)$. Substituting $H(z)$ and Eq. (33) into Eq. (18), we obtain the function $R(z)$ for RR of SF networks. As shown in Fig. 7, we find three regimes of coupling strength q :

- (i) When q is small ($q < q_c^e$), $R(z)$ is a monotonically increasing function of z , the system shows a second order phase transition, and the critical threshold p_c^{II} is obtained when $z \rightarrow 1$ which corresponds to $R(1) = \max\{R\} = \infty = 1/p_c^{II}$, i.e., $p_c^{II} = 0$.
- (ii) When q is larger, $q_c^e < q < q_{\max}$, $R(z)$ as a function of z shows a peak which corresponds to a sharp jump to a lower value of P_∞ at z_c with a hybrid transition, because $\max\{R\} \neq R(z_c)$, which is different from the ER case. Furthermore, the effective critical threshold (sharp jump) is $p_{ec}^I = 1/R(z_c)$, while for p below this sharp jump the system undergoes a smooth second order phase transition and the critical threshold is zero, similar to (i). Thus, when z is greater than some value, $R(z)$ increases with z again and reaches $\max\{R\}$ when $z \rightarrow 1$, which indicates that when p decreases below p_{ec}^I , P_∞ jumps as a first order to a finite small value and then decreases smoothly to 0 as p approaches 0;
- (iii) When q is above q_{\max} , $R(z)$ decreases with z first, and then increases with z , which corresponds to the system collapse.

Next we analyze the three regimes more rigorously.

- (i) When q is small ($q < q_c^e$), $R(z)$ is a monotonically increasing function of z , the maximum of $R(z_c)$ is obtained when $z_c \rightarrow 1$, which corresponds to $P_\infty = 0$,

$$\max\{R\} = \lim_{z \rightarrow 1} \frac{H(z) - 1}{z - 1} (1 - q)^m \doteq H'(1). \quad (34)$$

This is since when $M \rightarrow \infty$, $\max\{R\} \rightarrow \infty$, $p_c^{II} = 0$ when $q < q_c^e$.

- (ii) As q increases ($q \geq q_c^e$), $R(z)$ as a function of z shows a peak corresponding to $R(z) = R(z_c)$, $dR/dz = 0$ (smaller root has the physical meaning), where $R = R_c = 1/p_{ec}^I > 1$ corresponding to the effective critical threshold where P_∞ as a function of p shows an abrupt jump. Furthermore, we define

$$P_\infty^- = \lim_{p \rightarrow p_{ec}^I, p < p_{ec}^I} P_\infty(p), \quad (35)$$

and

$$P_{\infty}^{+} = \lim_{p \rightarrow p_{ec}^I, p > p_{ec}^I} P_{\infty}(p). \quad (36)$$

For the case of first order phase transition with a sharp jump, $P_{\infty}^{-} = 0$, but for the hybrid transition $P_{\infty}^{-} > 0$. After the sharp jump, P_{∞} decreases smoothly to 0 until $p = 0$. For the case of two partially interdependent SF networks see Zhou et. al. [54].

(iii) As q increases further ($q > q_{max}$), $\frac{dR(z)}{dz}$ at $z = 0$ becomes negative, thus the NetONet will collapse even when a single node is initially removed. So the maximum values of q is obtained as

$$\left. \frac{dR(z)}{dz} \right|_{z \rightarrow 0} = 0. \quad (37)$$

Using Eqs. (16), (18) and (37), we obtain

$$\begin{aligned} \frac{dR(z)}{dz} = & -\frac{G'(z)R(z)}{1-G(z)} - \frac{R(z)P'_{\infty}(z)}{P_{\infty}(z)} \\ & + \frac{2mR(z)}{1-q+\sqrt{(1-q)^2+4qP_{\infty}(z)}} \frac{qP'_{\infty}(z)}{\sqrt{(1-q)^2+4qP_{\infty}(z)}} \end{aligned} \quad (38)$$

When $q = q_{max}$, $P_{\infty}(z)|_{z \rightarrow 0} = 1$ and $P'_{\infty}(z)|_{z \rightarrow 0} = -1$, so we get

$$q_{max} = \frac{1}{m-1}. \quad (39)$$

Comparison between analytical and simulation results are shown in Fig. 8.

IV. FEEDBACK CONDITION

The above detailed analysis considers the case of no feedback condition since even for two fully interdependent networks with feedback condition (fb), both networks will completely collapse even if a single node fails. However, feedback condition can not destroy a network of partially interdependent networks when q is sufficiently small. For the case of feedback condition, Eqs. (15) become

$$x = p(qxg(x) - q + 1)^m. \quad (40)$$

Substituting $z = xf(x) + 1 - x$ and Eqs. (1)-(3) into Eq. (40) and eliminating x , we obtain

$$\frac{1}{p} = \frac{1-H(z)}{1-z} (1-q+qP_{\infty})^m \quad (41)$$

For ER networks, we obtain an equation for f

$$\ln f = \bar{k}p(1 - q - q\frac{\ln f}{\bar{k}})^{-m}(f - 1). \quad (42)$$

By substituting $P_\infty = -(\log f)/\bar{k}$, we determine the mutual percolation giant component for a RR network of ER networks with feedback condition,

$$P_\infty = p(1 - e^{-\bar{k}P_\infty})(1 - q + qP_\infty)^m. \quad (43)$$

Figure 9 shows numerical solutions of Eq. (43) for several q and m values, which are in excellent agreement with simulations, presented as symbols. These solutions imply that P_∞ as a function of p exhibits only a second order phase transition.

Indeed, from Eq. (43) and substituting $P_\infty = z$ ($z \in [0, 1]$), we obtain

$$R(z) = \frac{1}{p} = \frac{(1 - e^{-\bar{k}z})}{z}(1 - q + qz)^m, \quad (44)$$

and

$$\frac{dR(z)}{dz} = \frac{\bar{k}z - e^{\bar{k}z} + 1}{pz(e^{\bar{k}z} - 1)} - \frac{mq}{p(1 - q + qz)}. \quad (45)$$

Next, we prove that $R(z)$ is a decreasing function of z , i.e., $dR(z)/dz < 0$. It is easy to see

$$\frac{d}{dz}(\bar{k}z - e^{\bar{k}z} + 1) = \bar{k} - \bar{k}e^{\bar{k}z} \leq 0, \quad (46)$$

and the equal condition is satisfied only when $z = 0$, so $\bar{k}z - e^{\bar{k}z} + 1 < 0$. Thus we obtain that $R(z)$ is a monotonous decreasing function of z , which is very different from the no feedback condition. So the maximum of $R(z)$ is obtained only when $z \rightarrow 0$, which corresponds to the critical value of p_c ,

$$p_c = \frac{1}{\bar{k}(1 - q)^m}, \quad (47)$$

which is the same as Eq. (26). Thus, the second order threshold of no feedback p_c^{II} is the same as the feedback p_c , which is also shown in Fig. 10 (a). However, the feedback case is still more vulnerable than the no feedback case. Fig. 10 (b) and (c) show P_∞ for $p = 1$, i.e. the giant component in each network of the NetONet when there is no node failures, as a function of q . We can see that for the no feedback case, Fig. 10 (b), the system still has very large giant component left when both m and q are large, but for the feedback case,

there is not giant component when both m and q are large. This happens because of the single connected nodes and isolated nodes in each network [28].

Substituting $p_c \leq 1$ into Eq. (47), we obtain $\bar{k} \geq 1/(1-q)^m$ or $q \leq 1 - (1/\bar{k})^{1/m}$, which represents the minimum \bar{k} and maximum q for which a phase transition exists,

$$\bar{k}_{\min} = \frac{1}{(1-q)^m}, \quad (48)$$

and

$$q_{\max} = 1 - (1/\bar{k})^{1/m}. \quad (49)$$

Equations (48) and (49) demonstrate that the NetONet collapses when q and m are fixed and $\bar{k} < \bar{k}_{\min}$ and when m and \bar{k} are fixed and $q > q_{\max}$, i.e., there is no phase transition in these zones. However, q_{\max} of the feedback case is smaller than that of no feedback case shown in Fig. 11 (a), which shows that the feedback case is more vulnerable than the no feedback case. In Fig. 11 (b) we show that increasing \bar{k} or decreasing m will increase q_{\max} , i.e., increase the robustness of NetONet.

Next we study the feedback condition for the case of RR NetONet formed of RR networks of degree k . In this case, Eq. 43 becomes

$$1 - \left[1 - \frac{P_{\infty}}{p(1-q-qP_{\infty})} \right]^{\frac{1}{k}} = p \left\{ 1 - \left[1 - \frac{P_{\infty}}{p(1-q-qP_{\infty})} \right]^{\frac{k-1}{k}} \right\} (1-q+qP_{\infty})^m. \quad (50)$$

We find that the RR networks are very different from the ER networks, and the system shows first order phase transition for large q and a second order phase transition for small q as shown in Fig. 12.

V. DISCUSSION

In summary, we develop a general framework, Eqs. (10) and (11), for studying percolation in several types of NetONet of any degree distribution. We demonstrate our approach for a RR network of ER networks that can be exactly solved analytically, Eqs. (23) and for RR of SF networks for which the analytical expressions can be solved numerically. We find that q_{\max} and q_c^e exist, where a NetONet shows a second-order transition when $q < q_c^e$, a hybrid transition when $q_c^e < q < q_{\max}$, and that in all other cases there is no phase transition because all nodes in the NetONet spontaneously collapse. Thus the percolation theory of a single

network is a limiting case of a more general case of percolation of interdependent networks. Our results show that the percolation threshold and the giant component depend solely on the average degree of the ER network and the degree of the RR network, but not on the number of networks. These findings enable us to study the percolation of different topologies of NetONet. We expect this work to provide insights leading to further analysis of real data on interdependent networks. The benchmark models we present here can be used to study the structural, functional, and robustness properties of interdependent networks. Because, in real NetONets, individual networks are not randomly connected and their interdependent nodes are not selected at random, it is crucial that we understand many types of correlations existing in real-world systems and to further develop the theoretical tools studying all of them. Future studies of interdependent networks will need to focus on (i) an analysis of real data from many different interdependent systems and (ii) the development of mathematical tools for studying the vulnerability of real-world interdependent systems.

-
- [1] D. J. Watts & S. H. Strogatz , Nature **393**, 440 (1998).
 - [2] R. Albert, H. Jeong & A. L. Barabási , Nature **406**, 378 (2000).
 - [3] V. Rosato et al., Int. J. Crit. Infrastruct. **4**, 63 (2008).
 - [4] J. Peerenboom, R. Fischer & R. Whitfield, in Pro. CRIS/DRM/IIIT/NSF Workshop Mitigat. Vulnerab. Crit. Infrastruct. Catastr. Failures (2001).
 - [5] S. Rinaldi , J. Peerenboom & T. Kelly, IEEE Contr. Syst. Mag. **21**, 11-25 (2001).
 - [6] R. Albert & A. L. Barabási , Rev. Mod. Phys. **74**, 47 (2002).
 - [7] R. Cohen, K. Erez, D. ben-Avraham, S. Havlin, Phys. Rev. Lett. **85**, 4626 (2000); **86**, 3682 (2001).
 - [8] D. S. Callaway, M. E. J. Newman, S. H. Strogatz, D.J. Watts, Phys. Rev. Lett. **85**, 5468 (2000).
 - [9] M. E. J. Newman , SIAM Review **45**, 167 (2003).
 - [10] S. N. Dorogovtsev & J. F. F. Mendes, *Evolution of Networks: From Biological Nets to the Internet and WWW (Physics)* (Oxford Univ. Press, New York, 2003).
 - [11] C. Song et al., Nature **433**, 392 (2005).
 - [12] R. P. Satorras & A. Vespignani, *Evolution and Structure of the Internet: A Statistical Physics*

- Approach* (Cambridge Univ. Press, England, 2006).
- [13] G. Caldarelli & A. Vespignani, *Large scale Structure and Dynamics of Complex Webs* (World Scientific, 2007).
 - [14] A. Barrát , M. Barthélemy & A. Vespignani, *Dynamical Processes on Complex Networks* (Cambridge Univ. Press, England, 2008).
 - [15] R. Cohen & S. Havlin, *Complex Networks: Structure, Robustness and Function* (Cambridge Univ. Press, England, 2010).
 - [16] M. E. J. Newman, *Networks: An Introduction* (Oxford Univ. Press, New York, 2010).
 - [17] M. J. Pocock, D. M. Evans & J. Memmott, *Science* **335**,973–977 (2012).
 - [18] A. Bashan et. al. *Nature Communications* **3**, 702 (2012).
 - [19] K. Zhao, Kun & G. Bianconi, arXiv preprint arXiv:1210.7498.
 - [20] G. Li et. al. *Phys. Rev. Lett.* **104**, 018701, (2010).
 - [21] C. M Schneider,A. A Moreira, J. S Andrade, S. Havlin, H. J Herrmann, *Proc. Natl. Acad. Sci.* **108**, 3838–3841 (2011).
 - [22] S. V. Buldyrev et al., *Nature* **464**, 1025 (2010).
 - [23] R. Parshani, S. V. Buldyrev, S. Havlin, *Phys. Rev. Lett.* **105**, 048701 (2010).
 - [24] X. Huang et. al., *Phys. Rev. E* **83**, 055101 (2011).
 - [25] G. Dong et. al., *Phys. Rev. E* **85**, 016112 (2012).
 - [26] J. Shao, S. V. Buldyrev, S. Havlin, H. E. Stanley, *Phys. Rev. E* **83**, 036116 (2011).
 - [27] J. Gao, S. V. Buldyrev, S. Havlin & H. E. Stanley, *Phys. Rev. Lett.* **107**, 195701 (2011).
 - [28] J. Gao, S. V. Buldyrev, S. Havlin & H. E. Stanley, *Phys. Rev. E* **85**, 066134 (2012).
 - [29] J. Gao, S. V. Buldyrev, H. E. Stanley & S. Havlin, *Nature Physics* **8**, 40 (2011).
 - [30] A. Vespignani, *Nature* **464**, 984-985 (2010).
 - [31] E. A. Leicht & R. M. D’Souza, arXiv:cond-mat/0907.0894.
 - [32] R. G. Morris & M. Barthelemy, *Phys. Rev. Lett.* **109**, 128703 (2012).
 - [33] S. -W. Son, et al., *Europhys. Lett.* **97**, 16006 (2012).
 - [34] S.-M. Anna, S. M Ángeles, Boguñá, Marián, *Phys. Rev. E* **86**, 026106 (2012).
 - [35] S Gómez et al., *Phys. Rev. Lett.* **110**, 028701 (2013).
 - [36] J. Aguirre and D. Papo, J. Buldú, *Nature Physics* **9**, 230– 234 (2013).
 - [37] C. D Brummitt, R. M D’Souza, EA Leicht, *Proc. Natl. Acad. Sci.* **109**, 680–689 (2012).
 - [38] C. M Schneider et. al., *Scientific Reports*, in press (2013).

- [39] R. Parshani et. al., Euro. Phys. Lett. **92**, 68002 (2010).
- [40] Y. Hu, B. Ksherim, R. Cohen, S. Havlin, Phys. Rev. E **84**, 066116 (2011).
- [41] S. V. Buldyrev et al., Phys. Rev. E **83**, 016112 (2011).
- [42] Ian Dobson, Benjamin A. Carreras, Vickie E. Lynch, and David E. Newman, Chaos **17**, 026103 (2007)
- [43] M. Molloy & B. Reed, Combin. Probab. Comput. **7**, 295–305 (1998).
- [44] J. Shao et. al., Europhys. Lett. **84**, 48004 (2008).
- [45] M. E. J. Newman, S. H. Strogatz & D. J. Watts, Phys. Rev. E **64**, 026118 (2001).
- [46] M. E. J. Newman, Phys. Rev. E **66**, 016128 (2002).
- [47] J. Shao et. al., Phys. Rev. E **80**, 036105 (2009).
- [48] P. Erdős & A. Rényi, Publ. Math. **6**, 290 (1959).
- [49] P. Erdős & A. Rényi, Publ. Math. Inst. Hung. Acad. Sci. **5**, 17 (1960).
- [50] B. Bollobás , *Random Graphs* (Academic, London, 1985).
- [51] A. L. Barabási, & R. Albert, Science **286**, 509–512 (1999).
- [52] V. Colizza , A. Barrat, M. Barthélemy & A. Vespignani, Proc. Natl. Acad. Sci. **103**, 2015(2006).
- [53] D. Li, K. Kosmidis, A. Bunde & S. Havlin, Nature Physics **7**, 481–484 (2011).
- [54] D. Zhou, J. Gao, H. E. Stanley & S. Havlin, Phys. Rev. E, **87**, 052812 (2013).

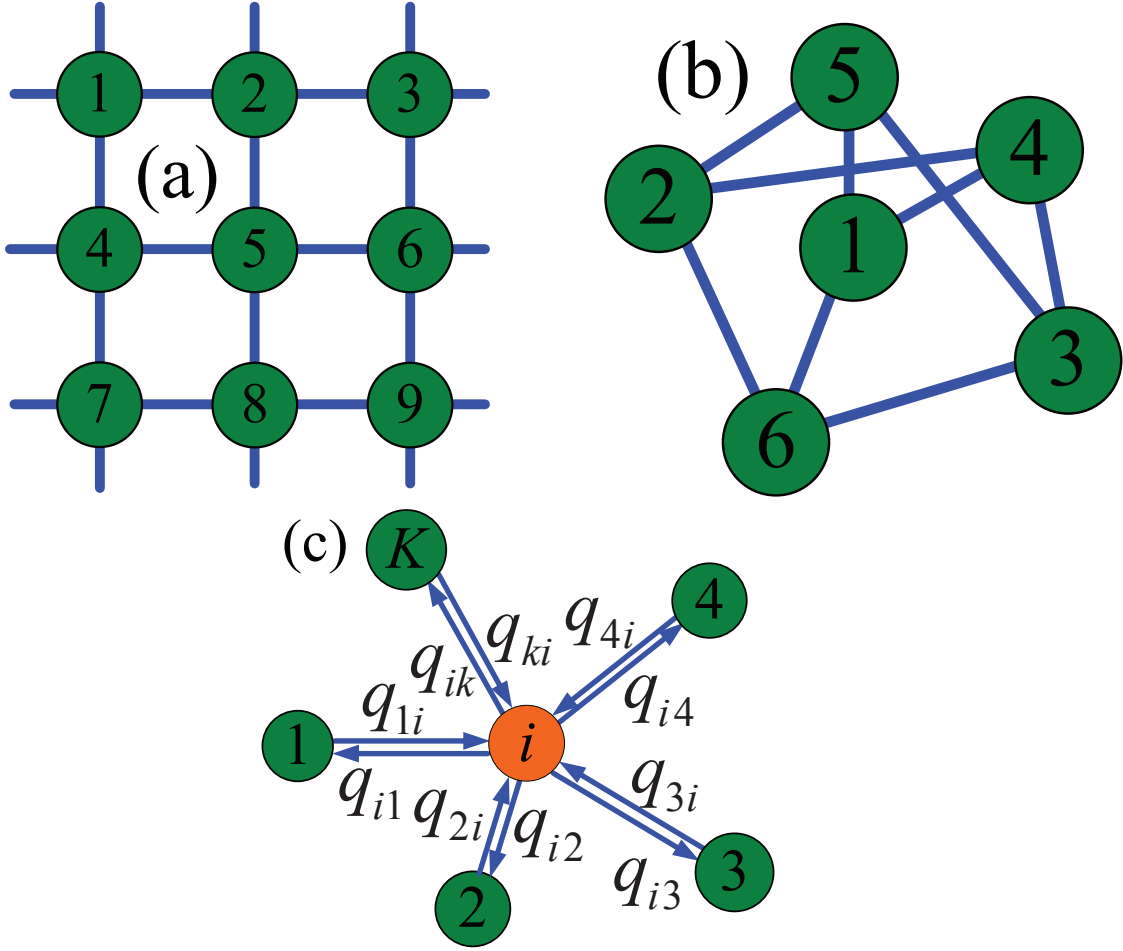


FIG. 1: **Illustration of regular and random regular (RR) NetONet of interdependent random networks.** (a) An example of a regular network, a lattice with periodic boundary condition composed of 9 interdependent networks represented by 9 circles. The degree of the NetONet is $m = 4$, i.e., each network depends on 4 networks. (b) A RR network composed of 6 interdependent networks represented by 6 circles. The degree of the NetONet is $m = 3$, i.e., each network depends on 3 networks. The analytical results for the NetONet [Eqs. (15) and (17)] are exact and the same for both cases (a) and (b). (c) Schematic representation of the dependencies of the networks. Circles represent networks in the NetONet, and the arrows represent the partially interdependent pairs. For example, a fraction of q_{3i} of nodes in network i depends on nodes in network 3. Pairs of networks which are not connected by dependency links do not have nodes that directly depend on each other.

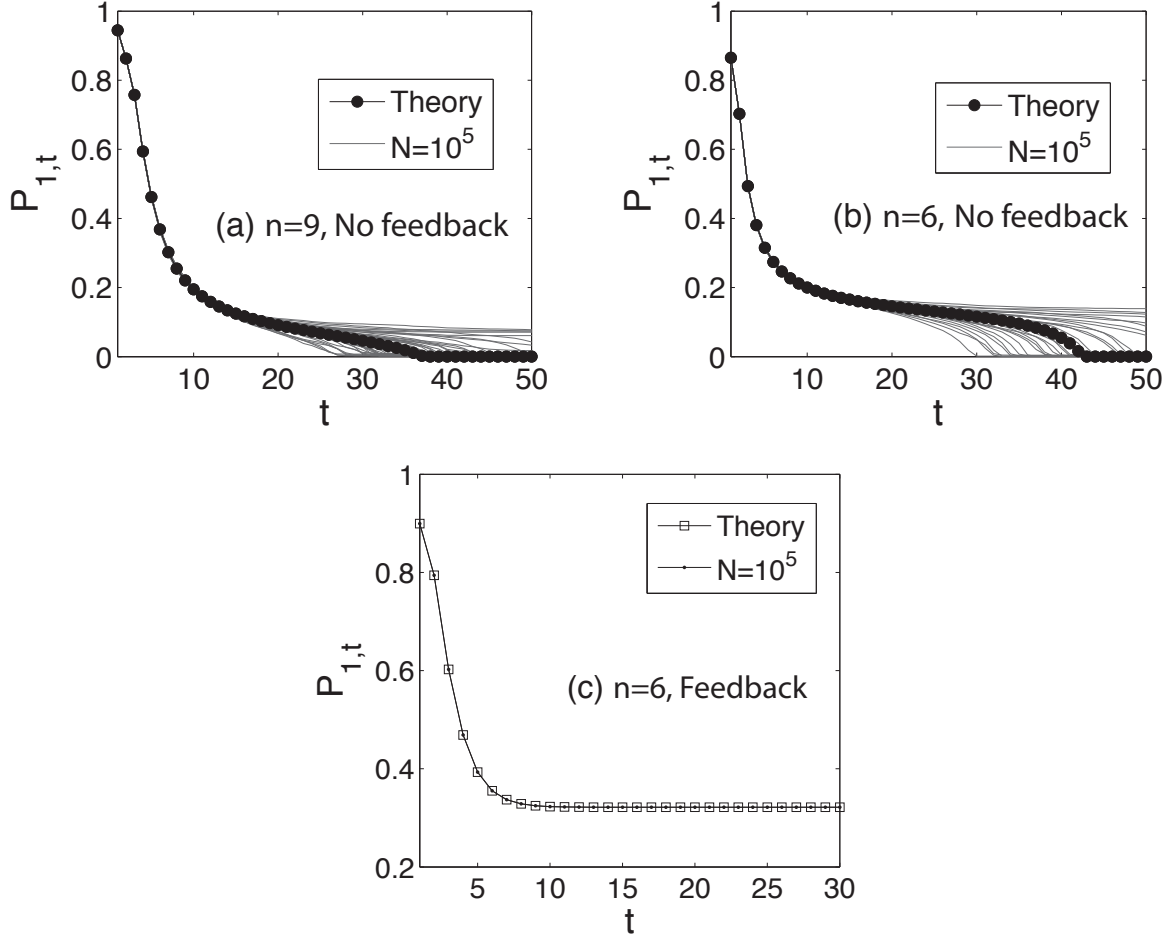


FIG. 2: (a) Simulation results compared with theory of the giant component of network 1, $P_{1,t}$, after t cascading failures for the lattice NetONet composed of 9 ER networks shown in Fig. 1(a). For each network in the NetONet, $N = 10^5$, $m = 4$ and $\bar{k} = 8$, and $q = 0.4 > q_c \doteq 0.382$ (predicted by Eq. (30)). The chosen value of p is $p = 0.945$, and the predicted threshold is $p_c^I = 0.952$ (from Eq. (27)). (b) Simulations compared to theory of the giant component, $P_{t,1}$, for the random regular NetONet composed of 6 ER networks shown in Fig. 1(b) with the no feedback condition. For each network in the NetONet, $N = 10^5$, $m = 3$, $\bar{k} = 8$, $q = 0.49 > q_c \doteq 0.4313$ (predicted by Eq. (30)), and for $p = 0.866 < p_c^I \doteq 0.8696$ (from Eq. (27)). (c) Simulations compared to theory of the giant component, $P_{1,t}$, for the random regular NetONet composed of 6 ER networks shown in Fig. 1(b) with the feedback condition. For each network in the NetONet, $N = 10^5$, $m = 3$, $\bar{k} = 8$, $q = 0.4 < q_{\max} = 0.5$ (predicted by Eq. (49)), and for $p = 0.9 > p_c \doteq 0.5787$ (from Eq. (47)). The results are averaged over 20 simulated realizations of the giant component left after t stages of the cascading failures which is compared with the theoretical prediction of Eq. (9).

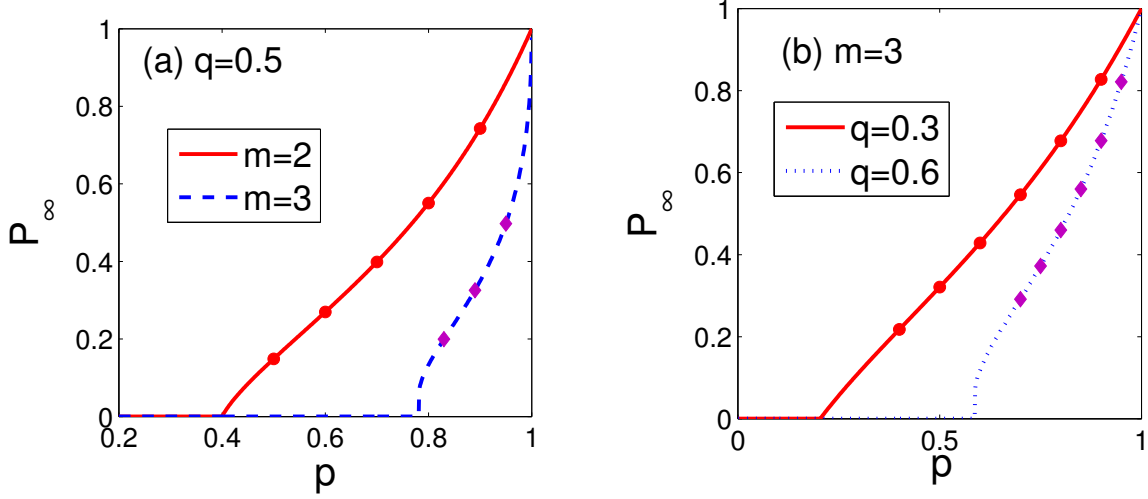


FIG. 3: The giant component for an RR network of ER networks, P_∞ , as a function of p , for ER networks with average degree $\bar{k} = 10$, (a) for two different values of m and $q = 0.5$, (b) for two different values of q and $m = 3$. The curves in (a) and (b) are obtained using Eq. (23) and are in excellent agreement with simulations. The points symbols are obtained from simulations by averaging over 20 realizations for $N = 2 \times 10^5$. In (a), simulation results are shown as circles ($n = 6$) for $m = 2$ and as diamonds ($n = 12$) for $m = 3$. These simulation results support our theoretical result, Eq. (23), which is indeed independent of number of networks n .

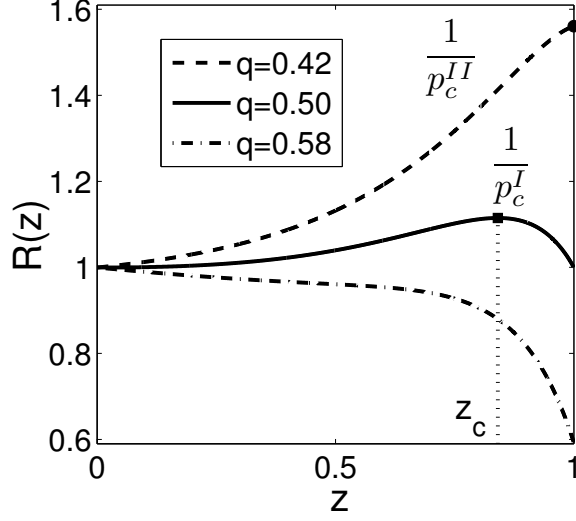


FIG. 4: Plot of $R(z)$ as a function of z for an RR network of ER networks, for different values of q when $m = 3$ and $\bar{k} = 8$. All the lines are produced using Eq. (24). The symbols \bullet and \blacksquare show the critical thresholds p_c^{II} when $q = 0.42 < q_c = 0.4313$ and p_c^I when $q = 0.5 < q_{\max} = 0.5462$. These critical thresholds coincide with the results in Fig. 3(a). The dashed dotted line shows that when $q = 0.58 > q_{\max}$ the function (24) has no solution for $p = 1$, which corresponding to the case of complete collapse of the NetOnet.

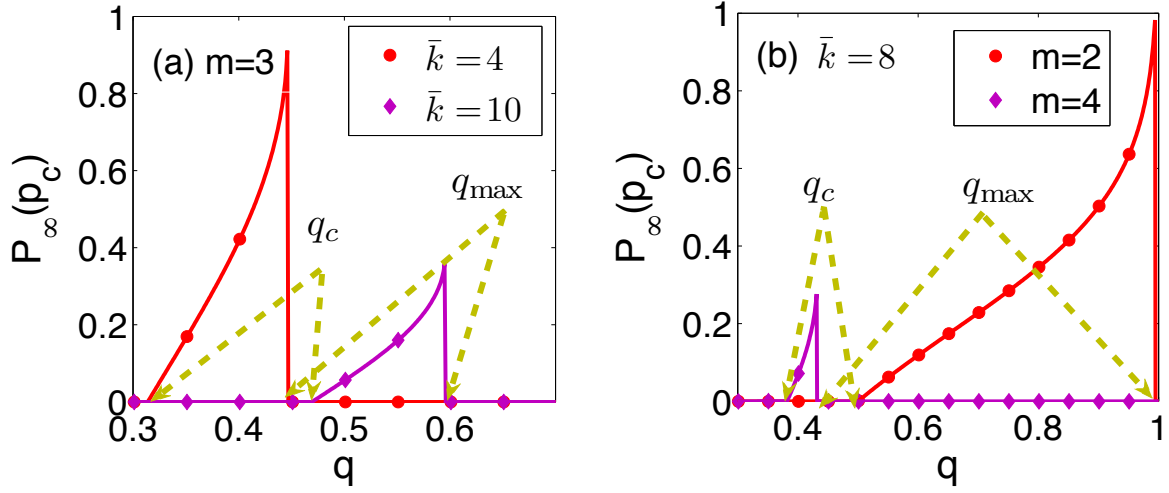


FIG. 5: The giant component for an RR NetONet formed of ER networks at p_c , $P_\infty(p_c)$, as a function of q . The curves are (a) for $m = 3$ and two different values of \bar{k} , and (b) for $\bar{k} = 8$ and two different values of m . The curves are obtained using Eqs. (23) and (26) and are in excellent agreement with simulations (symbols). Panels (a) and (b) show the location of q_{\max} and q_c for two values of m . Between q_c and q_{\max} the transition is first order represented by $P_\infty(p_c) > 0$. For $q < q_c$ the transition is second order since $P_\infty(p_c) = 0$ and for $q > q_{\max}$ the NetONet collapses ($P_\infty(p_c) = 0$) and there is no phase transition ($p_c = 1$).

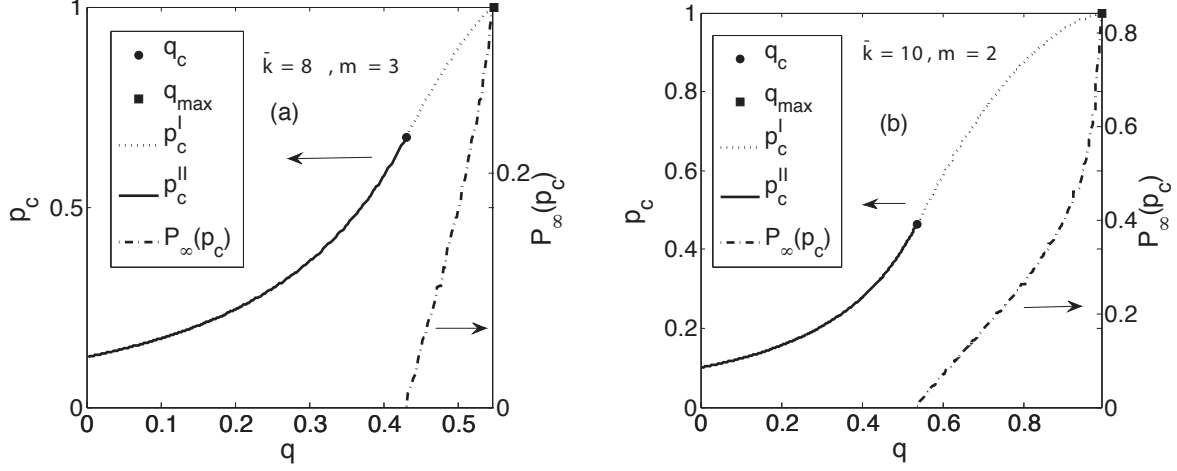


FIG. 6: The phase diagram for RR network of ER networks, (a) for $m = 3$ and $\bar{k} = 8$, (b) for $m = 2$ and $\bar{k} = 10$. The solid curves show the second order phase transition (predicted by Eq. (30)) and the dashed-dotted curves show the first order phase transition, leading $P_\infty(p_c)$ at q_c from zero to non-zero values (the rhs axis). As m decreases and \bar{k} increases, the region for $P_\infty > 0$ increases, showing a better robustness. The circle shows the tri-critical point q_c , below which second order transition occurs and above which a first order transition occurs. The square shows the critical point q_{\max} , above which the NetONet completely collapse even when $p = 1$.

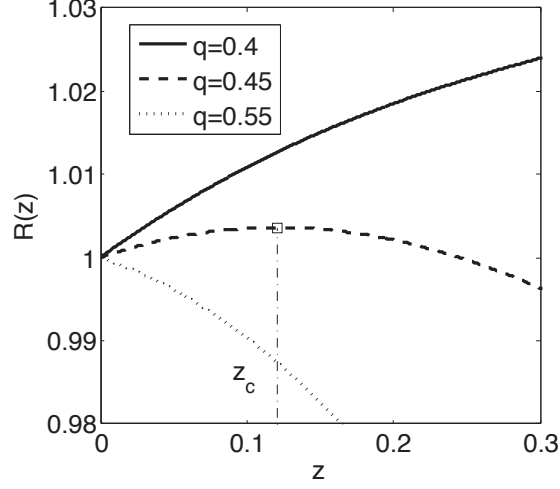


FIG. 7: For RR NetONet formed of SF networks $R(z)$ as a function of z for different values of q when $m = 3$, $\lambda = 2.3$, $s = 2$ and $M = 1000$. (i) When q is small ($q = 0.4 < q_c$), $R(z)$ is a monotonically increasing function of z , the system shows a second order phase transition. (ii) When q is larger ($q_c < q = 0.45 < q_{\max}$), $R(z)$ as a function of z shows a peak at z_c which corresponds to a hybrid phase transition. The square symbol represents the critical point of the sharp jump (z_c). (iii) When q is large enough ($q = 0.55 > q_{\max}$), $R(z)$ decreases with z first, and then increases with z , which corresponds the system collapses.

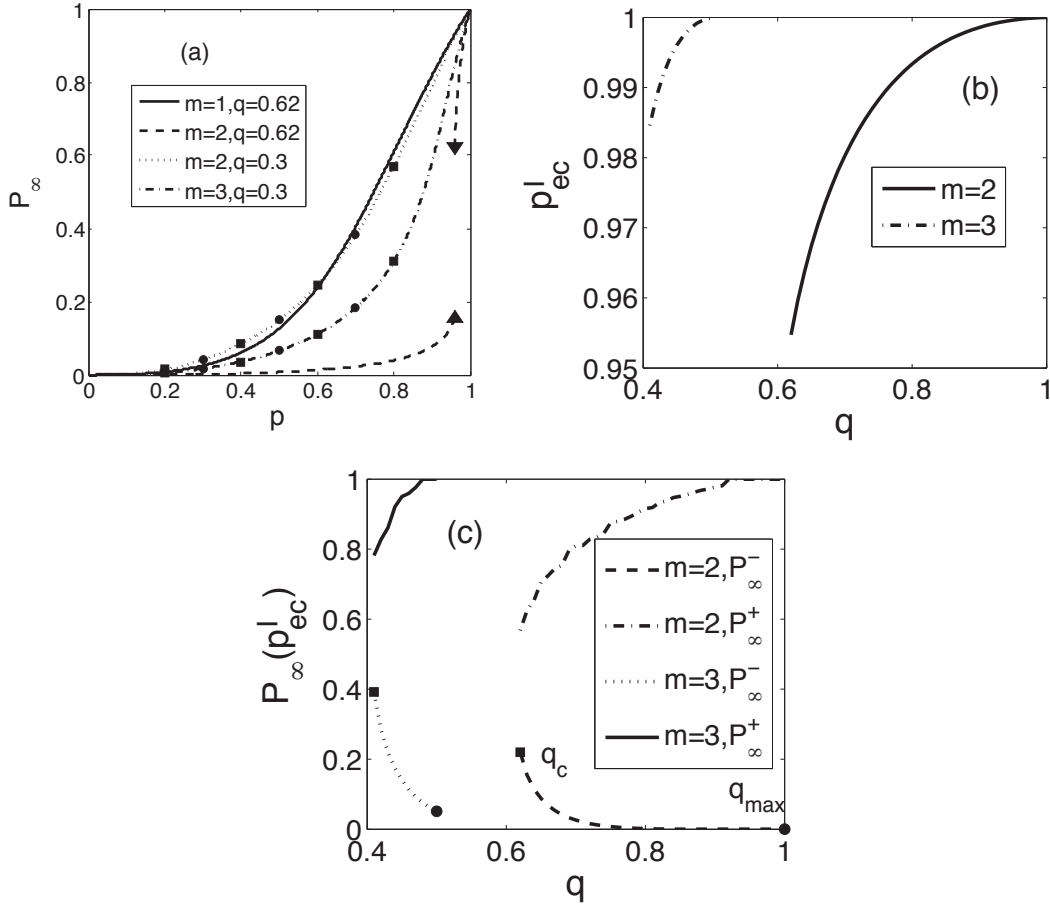


FIG. 8: Results for a RR network formed of SF networks. (a) The giant component P_∞ as a function of p for different values of m and q for $\lambda = 2.5$. (b) The critical threshold p^I_{ec} and (c) the corresponding giant component at the threshold $P_\infty(p^I_{ec})$ as a function of coupling strength q for $m = 2$ and $m = 3$. The symbols in (a) represent simulation results, obtained by averaging over 20 realizations for $N = 2 \times 10^5$ and number of networks $n = 6$ (squares) and $n = 4$ (circles). The lines are the theoretical results obtained using Eqs. (17) and (1)-(3). We can see in (a) that the system shows a hybrid phase transition for $m = 2$ and $q_c^e < q = 0.62 < q_{\max} = 1/(m - 1)$. When $q < q_c^e$ the system shows a second order phase transition and the critical threshold is $p_c^{II} = 0$. However, in the simulation when p is small (but not zero) $P_\infty = 0$. This happens because $p_c^{II} = 0$ is valid only when the network size $N = \infty$ and $M = \infty$, but in simulations we have finite systems. Furthermore, when $q_c^e < q < q_{\max}$ the system shows a hybrid transition shown in (a) and (c), and when $q > q_{\max}$ all the networks collapse even if one node fails. We call this hybrid transition because $P_\infty^- > 0$, which is different from the case of ER networks with first order phase transition where $P_\infty^- = 0$.

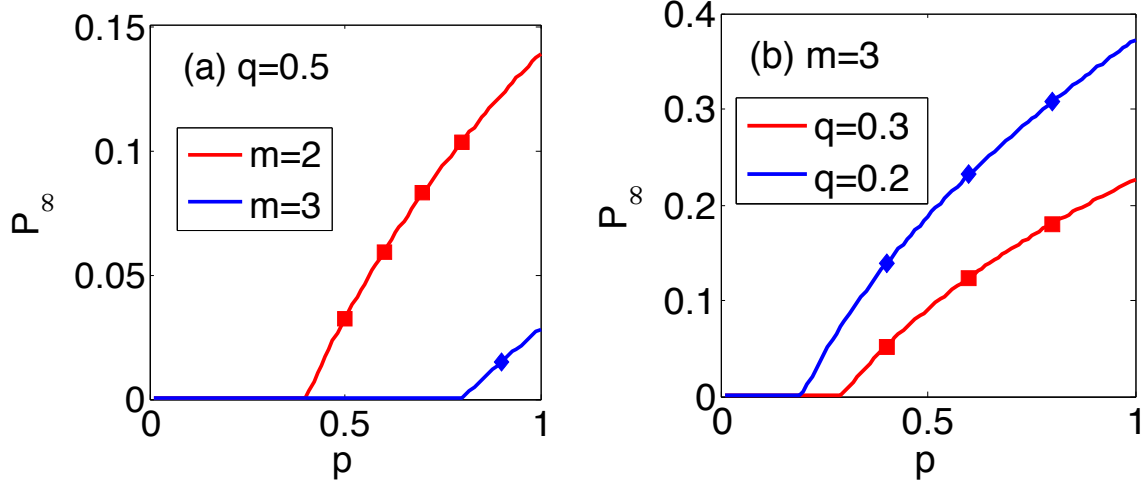


FIG. 9: The giant component for an RR network of ER networks with feedback condition, P_∞ , as a function of p for ER average degree $\bar{k} = 10$, for different values of m when $q = 0.5$ (a) and for different values of q when $m = 3$. The curves in (a) and (b) are obtained using Eq. (43) and are in excellent agreement with simulations. The points symbols are obtained from simulations of Fig. 1(b) topology when $m = 3$ and $n = 6$ networks forming a circle when $m = 2$ by averaging over 20 realizations for $N = 2 \times 10^5$. The absence of first order regime in NetONet formed of ER networks is due to the fact that at the initial stage nodes in each network are interdependent on isolated nodes (or clusters) in the other network. However, if only nodes in the giant components of both networks are interdependent, all three regimes, second order, first order and collapse will occur, like in the case of RR NetONet formed of RR networks (see Eq. (50) and Fig. 12).

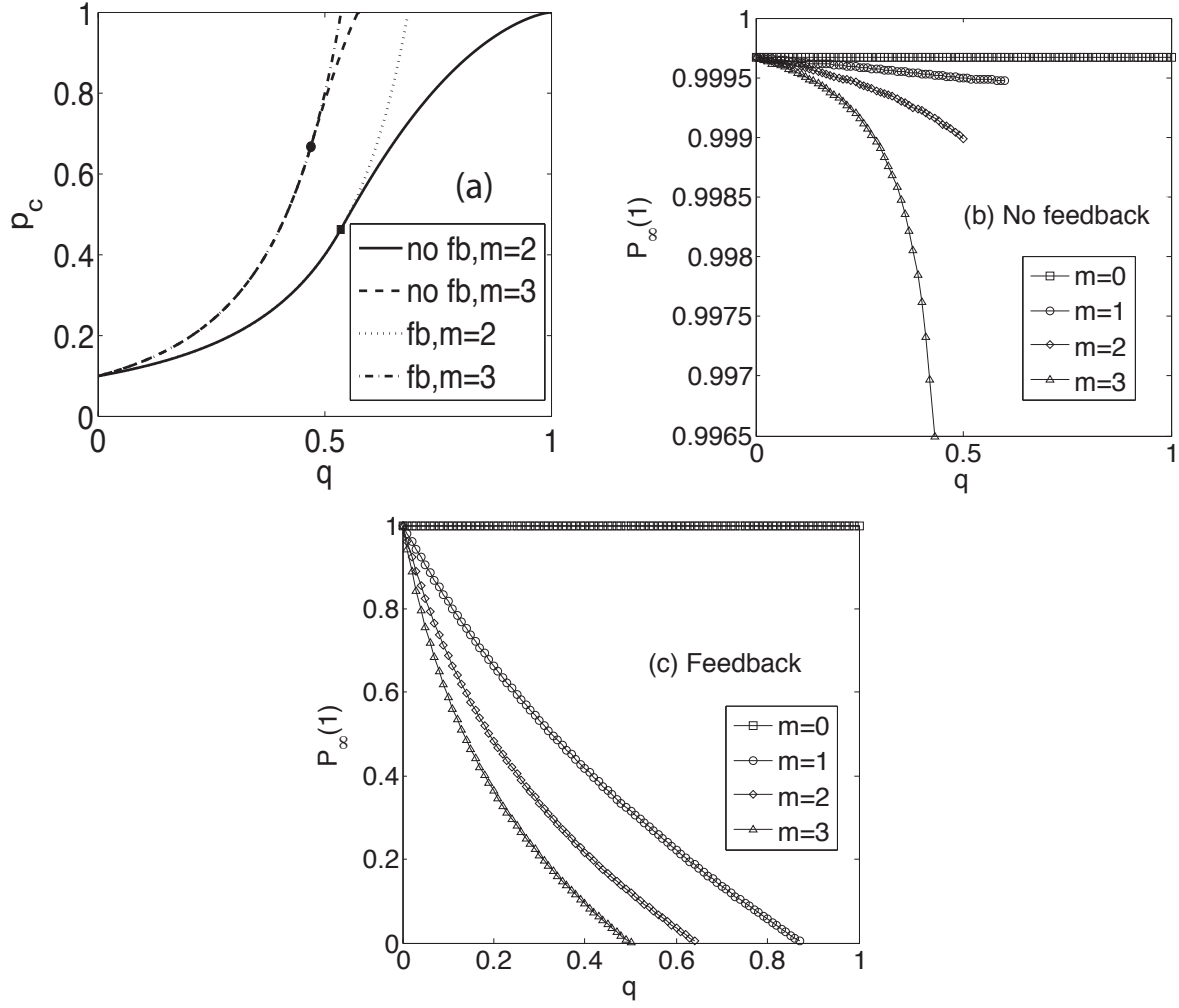


FIG. 10: (a) p_c as a function of q for both no feedback condition and feedback condition when $\bar{k} = 10$. For no feedback condition, the parts of curves below the symbols show p_c^{II} and above the symbols show p_c^I . For the feedback condition, they only have the p_c of second order, and p_c^{II} for the no feedback case is equal to p_c of the feedback case, but this does not mean that these two cases have equal vulnerability. $P_\infty(1)$ as a function of q for different values of m when $\bar{k} = 8$ with (b) no feedback condition and (c) feedback condition. When $q = 0$, $P_\infty(1) = 1 - \exp(-\bar{k})$ for all m and both feedback and no feedback cases. Comparing (b) and (c), we can see that the feedback case is much more vulnerable than the no feedback condition, because $P_\infty(1)$ of no feedback case is much less than that of feedback case.

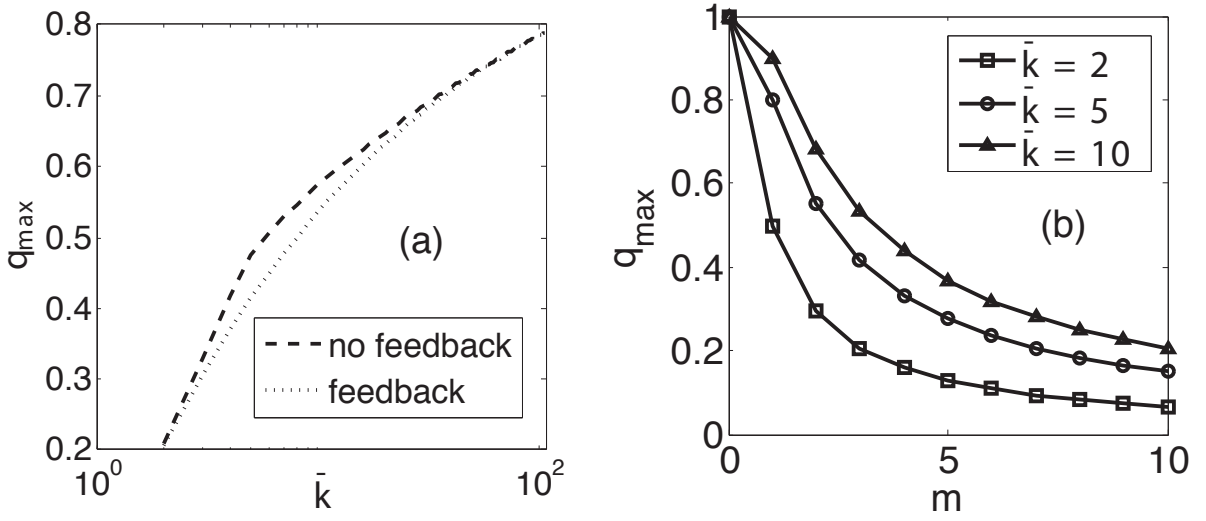


FIG. 11: (a) The maximum value of coupling strength q_{\max} as a function of \bar{k} for the case of feedback condition and no feedback condition when $m = 3$. We can see that q_{\max} of no feedback case is larger than that of the feedback case, which indicate that the no feedback case is more robust compared to the feedback case. (b) The maximum value of coupling strength q_{\max} as a function of m with the feedback condition for different values of \bar{k} , which shows that increasing \bar{k} or decreasing m will increase q_{\max} , i.e., increase the robustness of NetONet.

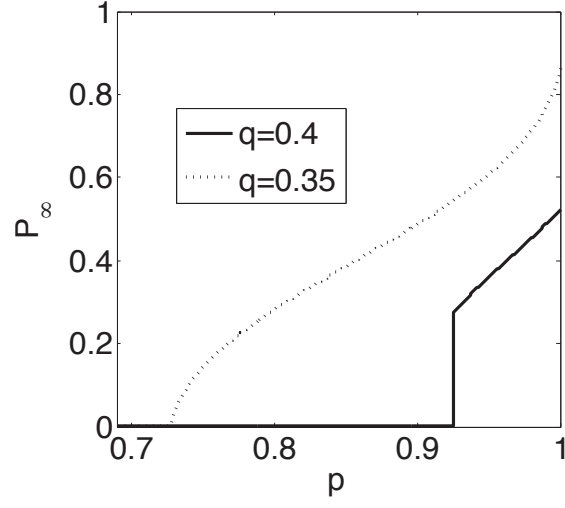


FIG. 12: The giant component for an RR NetONet formed of RR networks with feedback condition, P_∞ , as a function of p for RR of degree $k = 6$ and $m = 3$, for two different values of q . The curves are obtained using Eq. (50), which shows a first order phase transition when q is large but a second order phase transition when q is small.